

Multi-year record of atmospheric mercury at Dumont d'Urville, East Antarctic coast: continental outflow and oceanic influences

Hélène Angot¹, Iris Dion¹, Nicolas Vogel¹, Michel Legrand^{1, 2}, Olivier Magand^{2, 1}, Aurélien Dommergue^{1, 2}

¹Univ. Grenoble Alpes, Laboratoire de Glaciologie et Géophysique de l'Environnement (LGGE), 38041 Grenoble, France

²CNRS, Laboratoire de Glaciologie et Géophysique de l'Environnement (LGGE), 38041 Grenoble, France

Correspondence to: A. Dommergue (aurelien.dommergue@univ-grenoble-alpes.fr)

Abstract

Under the framework of the Global Mercury Observation System (GMOS) project, a 3.5-year record of atmospheric gaseous elemental mercury (Hg(0)) has been gathered at Dumont d'Urville (DDU, 66°40'S, 140°01'E, 43 m above sea level) on the East Antarctic coast. Additionally, surface snow samples were collected in February 2009 during a traverse between Concordia Station located on the East Antarctic plateau and DDU. The record of atmospheric Hg(0) at DDU reveals particularities that are not seen at other coastal sites: a gradual decrease of concentrations over the course of winter, and a daily maximum concentration around midday in summer. Additionally, total mercury concentrations in surface snow samples were particularly elevated near DDU (up to 194.4 ng L⁻¹) as compared to measurements at other coastal Antarctic sites. These differences can be explained by the more frequent arrival of inland air masses at DDU than at other coastal sites. This confirms the influence of processes observed on the Antarctic plateau on the cycle of atmospheric mercury at a continental scale, especially in areas subject to recurrent katabatic winds. DDU is also influenced by oceanic air masses and our data suggest that the ocean plays a dual role on Hg(0) concentrations. The open ocean may represent a source of atmospheric Hg(0) in summer whereas the sea-ice surface may provide reactive halogens in spring that can oxidize

30 Hg(0). This paper also discusses implications for coastal Antarctic ecosystems and for the
31 cycle of atmospheric mercury in high southern latitudes.

32

33 **1 Introduction**

34 The Antarctic continent is one of the last near-pristine environments on Earth and still
35 relatively unaffected by human activities. Except for pollutants released from Antarctic
36 Research stations (e.g., Hale et al., 2008; Chen et al., 2015) and by marine and air-borne
37 traffic (Shirsat and Graf, 2009), only the long-lived atmospheric contaminants reach this
38 continent situated far from anthropogenic pollution sources. With an atmospheric lifetime on
39 the order of one year (Lindberg et al., 2007), gaseous elemental mercury (Hg(0)) is efficiently
40 transported worldwide. Hg(0) is the most abundant form of mercury in the atmosphere
41 (Lindberg and Stratton, 1998). It can be oxidized into highly-reactive and water-soluble
42 gaseous divalent species (Hg(II)) – that can bind to existing particles and form particulate
43 mercury (Hg(p)) – leading to the deposition of reactive mercury onto various environmental
44 surfaces through wet and dry processes (Lindqvist and Rodhe, 1985; Lin and Pehkonen,
45 1999). Upon deposition, Hg(II) can be reduced and reemitted back to the atmosphere as Hg(0)
46 (Schroeder and Munthe, 1998). Assessing mercury deposition and reemission pathways
47 remains difficult due to an insufficient understanding of the involved physic-chemical
48 processes.

49 Only sparse measurements of atmospheric mercury have been performed in Antarctica and
50 there are still many gaps in our understanding of its cycle at the scale of this vast continent (~
51 14 million km²) (Dommergue et al., 2010). To date, observations were made over one year at
52 the coastal site of Neumayer (NM, Ebinghaus et al., 2002; Temme et al., 2003) and during
53 summer campaigns at Terra Nova Bay (TNB, Sprovieri et al., 2002) and McMurdo (MM,
54 Brooks et al., 2008b). More recently, multi-year records have been obtained at Troll (TR)
55 situated approximately 220 km from the coast at 1275 m a.s.l. (Pfaffhuber et al., 2012) and
56 Concordia Station located at Dome C (denoted DC, 3220 m a.s.l.) (Angot et al., 2016). Under
57 the framework of the GMOS project (Global Mercury Observation System, www.gmos.eu),
58 atmospheric monitoring of Hg(0) has been implemented at Dumont d’Urville (DDU) located
59 in Adélie Land (Fig. 1) and we here report the obtained 3.5-year record of atmospheric Hg(0)
60 that represents the first multi-year record of Hg(0) available for the East Antarctic coast. In
61 this paper, the Hg(0) record from DDU is discussed in terms of influence of marine versus

62 inland air masses, and compared to records available at other coastal (NM, TNB, MM) or
63 near-coastal (TR) stations. In parallel, total mercury was determined in surface snow samples
64 collected during a traverse between DC and DDU in February 2009. These results provide
65 new insight into the transport and deposition pathways of mercury species in East Antarctica.

66

67 **2 Experimental Section**

68 **2.1 Sampling site and prevailing meteorological conditions**

69 From January 2012 to May 2015, Hg(0) measurements were performed at DDU station
70 located on a small island (Ile des Pétrels) about one km offshore from the Antarctic mainland.
71 A detailed description of the sampling site (“Labo 3”) has been given by Preunkert et al.
72 (2013) while the climatology of this coastal station has been detailed by König-Langlo et al.
73 (1998). The average surface air temperature ranges from -1 °C in January to -17 °C in winter,
74 with a mean annual temperature of -12 °C. The annual mean surface wind speed is 10 m s⁻¹,
75 with no clear seasonal variations. Due to the strong katabatic effects, the most frequent
76 surface wind direction is 120°E-160°E.

77 **2.2 Methods**

78 **2.2.1 Hg(0) measurements**

79 Hg(0) measurements were performed using a Tekran 2537B (Tekran Inc., Toronto, Canada).
80 The sampling resolution ranged from 10 to 15 minutes with a sampling flow rate of 1.0 L min⁻¹.
81 Concentrations are reported here as hourly averages and are expressed in nanograms per
82 cubic meter at standard temperature and pressure (273.15 K, 1013.25 hPa). Setting a 0.2 µm
83 PTFE filter and a 10 m long unheated sampling line on the front of the analyzer inlet, we
84 assume that mainly Hg(0) (instead of total gaseous mercury, defined as the sum of gaseous
85 mercury species) was efficiently collected and subsequently analyzed by the instrument
86 (Steffen et al., 2002; Temme et al., 2003; Steffen et al., 2008).

87 External calibrations were performed twice a year by injecting manually saturated mercury
88 vapor taken from a temperature-controlled vessel, using a Tekran 2505 mercury vapor
89 calibration unit and a Hamilton digital syringe, and following a strict procedure adapted from
90 Dumarey et al. (1985). As described by Angot et al. (2014), fortnightly to monthly routine
91 maintenance operations were performed. A software program was developed at the LGGE

92 (Laboratoire de Glaciologie et Géophysique de l'Environnement) following quality control
93 practice commonly applied in North American networks (Steffen et al., 2012). Based on
94 various flagging criteria (Munthe et al., 2011; D'Amore et al., 2015), it enabled rapid data
95 processing in order to produce clean time series of Hg(0). According to the instrument
96 manual, the detection limit is 0.10 ng m^{-3} (Tekran, 2011).

97 **2.2.2 Snow sampling and analysis**

98 Eleven surface snow samples (the upper 3 cm) were collected during a traverse between DC
99 and DDU conducted in February 2009. As described by Dommergue et al. (2012), samples
100 were collected using acid cleaned PTFE bottles and clean sampling procedures. After
101 sampling, samples were stored in the dark at $-20 \text{ }^{\circ}\text{C}$. Field blanks were made by opening and
102 closing a bottle containing mercury-free distilled water. Total mercury (Hg_{tot}) in snow
103 samples was analyzed using a Tekran Model 2600. Hg_{tot} includes species such as HgCl_2 ,
104 $\text{Hg}(\text{OH})_2$, HgC_2O_4 , stable complexes such as HgS and $\text{Hg}(\text{II})$ bound to sulfur in humic
105 compounds, or some organomercuric species (Lindqvist and Rodhe, 1985). The instrument
106 was calibrated with the NIST SRM-3133 mercury standard. Quality assurance and quality
107 control included the analysis of analytical blanks, replicates, and internal standards (Reference
108 Waters for mercury: HG102-2 at 22 ng/L from Environment Canada). The limit of
109 quantification – calculated as 10 times the standard deviation of a set of 3 analytical blanks –
110 was 0.3 ng L^{-1} and the relative accuracy $\pm 8\%$.

111 Surface snow samples collected during traverses may have limited spatial and temporal
112 representativeness given the variability of chemical species deposition onto the snow surface,
113 and the occurrence of either fresh snowfall or blowing snow. The (in)homogeneity of surface
114 snow samples was investigated at MM by Brooks et al. (2008b). Surface (3-5 cm) snow
115 samples were collected daily ($n = 14$) at different snow patches. Hg_{tot} concentrations averaged
116 $67 \pm 21 \text{ ng L}^{-1}$. This result indicates that the spatial and temporal representativeness of surface
117 snow samples collected in Antarctica can be satisfactory and gives us confidence that spatial
118 differences in Hg_{tot} concentrations reported in section 3.2.2 are not due to samples
119 inhomogeneity.

120 **2.2.3 Ancillary parameters**

121 O_3 was continuously monitored with a UV absorption monitor (Thermo Electron Corporation
122 model 49I, Franklin, Massachusetts) (Legrand et al., 2009). Collected at 15-s intervals, the
123 data are reported here as hourly averages.

124 Back trajectories were computed using the HYSPLIT (Hybrid Single-Particle Lagrangian
125 Integrated Trajectory) model (Draxler and Rolph, 2013). Meteorological data from Global
126 Data Assimilation Process (available at <ftp://arlftp.arlhq.noaa.gov/pub/archives/gdas1>) were
127 used as input, and the model was run every hour in backward mode for 5 days at 0, 200, and
128 500 m above the model ground level. Three typical situations prevail at DDU: strong
129 katabatic winds flowing out from the Antarctic ice sheet situated south of the station, pure
130 marine air masses, or continental/marine mixed air masses with easterly winds due to the
131 arrival near the site of low-pressure systems (König-Langlo et al., 1998). Oceanic origin was
132 attributed to air masses having traveled at least 1 day over the ocean and less than 3 days out
133 of 5 over the high-altitude Antarctic plateau. Conversely, plateau origin refers to air masses
134 having traveled at least 3 days over the high-altitude Antarctic plateau and less than 1 day out
135 of 5 over the ocean. Finally, mixed origin refers to air masses having traveled less than 1 and
136 3 days out of 5 over the ocean and the high-altitude Antarctic plateau, respectively. It should
137 be noted that uncertainties associated with calculated backward trajectories arise from
138 possible errors in input meteorological fields and numerical methods (Yu et al., 2009), and
139 increase with time along the way (Stohl, 1998). According to Jaffe et al. (2005), back
140 trajectories only give a general indication of the source region. Despite these limitations, back
141 trajectories remained very similar at the three levels of altitude arrival at the site and we only
142 use here those arriving at the model ground level. This method also gave consistent results
143 with respect to the origin of various chemical species including O₃ (Legrand et al., 2009),
144 HCHO (Preunkert et al., 2013), NO₂ (Grilli et al., 2013), and sea-salt aerosol (Legrand et al.,
145 2016a).

146 **2.3 Local contamination**

147 Pollution plumes due to the station activities (e.g., combustion, vehicular exhaust)
148 occasionally reached the sampling site. Such local pollution events can be easily identified for
149 instance by the fast decrease of O₃ or increase of HCHO mixing ratios (Legrand et al., 2009;
150 Preunkert et al., 2013). We used a criterion based on wind direction and sudden drops of O₃
151 mixing ratios to filter the raw data (i.e., collected at 5 min intervals) and discard Hg(0) data
152 impacted by local pollution. Raw Hg(0) data above 1.60 ng m⁻³, corresponding to the mean +
153 3 standard deviation, obtained when the wind was blowing from 30°W to 70°E (i.e., the sector
154 where main station activities are located), and accompanied by a drop of O₃ were discarded

155 from the data set. Using this criterion, only 0.1% of raw Hg(0) data was discarded, the Hg(0)
156 record being very weakly impacted by pollution plumes.

157

158 **3 Results and Discussion**

159 The record of atmospheric Hg(0) from January 2012 to May 2015 is displayed in Fig. 2.
160 Hourly-averaged Hg(0) concentrations ranged from 0.10 to 3.61 ng m⁻³, with an average value
161 of 0.87 ± 0.23 ng m⁻³ (mean ± standard deviation). This mean annual Hg(0) concentration is
162 in good agreement with the value of 0.93 ± 0.19 ng m⁻³ (4-year average) reported by
163 Pfaffhuber et al. (2012) at TR, but lower than the concentration of 1.06 ± 0.24 ng m⁻³ (12-
164 month average) reported by Ebinghaus et al. (2002) at NM. While the same device was used
165 at the three stations, the measurements may target different mercury species depending on
166 their configuration (e.g., heated/unheated sample line). The difference between total gaseous
167 mercury and Hg(0) data can be rather substantial since gaseous oxidized mercury (Hg(II))
168 concentrations of up to ~ 0.30 ng m⁻³ were reported in spring/summer at several coastal
169 Antarctic stations (Sprovieri et al., 2002; Temme et al., 2003; Brooks et al., 2008b). To
170 allow a more accurate comparison of data available at the various Antarctic stations, more
171 harmonized sampling protocols are needed. Seasonal boundaries have been defined as
172 follows: summer refers to November-February, fall to March-April, winter to May-August,
173 and spring to September-October. Though being arbitrary, this dissection was done by
174 considering the time period over which the halogen chemistry (September-October) or the
175 OH/NO_x chemistry (November-February) is dominant at DDU (see sections 3.1.2 and 3.2.2).
176 The mechanisms which cause the seasonal variation of Hg(0) concentrations are discussed in
177 the following sections.

178 **3.1 From winter darkness to spring sunlight**

179 **3.1.1 Continental outflow and advection from lower latitudes in winter**

180 A gradual 20% decrease in Hg(0) concentrations from 0.89 ± 0.09 in average in May to 0.72
181 ± 0.10 ng m⁻³ in August (Fig. 3a) was observed at DDU. Conversely, concentrations remained
182 rather stable at NM and TR in winter with mean values of 1.15 ± 0.08 and 1.00 ± 0.07 ng m⁻³,
183 respectively (Ebinghaus et al., 2002; Pfaffhuber et al., 2012). Pfaffhuber et al. (2012)
184 suggested that this stability of Hg(0) concentrations at TR is related to a lack of oxidation
185 processes during the polar night.

186 A local reactivity at DDU – absent at other coastal stations – seems unlikely. Angot et al.
187 (2016) showed evidence of a gradual 30% decrease of Hg(0) concentrations at DC at the same
188 period of the year (Fig. 3a), probably due to a gas-phase oxidation, heterogeneous reactions,
189 or dry deposition of Hg(0) onto the snowpack. Since the decreasing trend observed in winter
190 is less pronounced at DDU than at DC, it most likely results from reactions occurring within
191 the shallow boundary layer on the Antarctic plateau, subsequently transported toward the
192 coastal margins by katabatic winds. This assumption is supported by the HYSPLIT model
193 simulations showing prevalence in winter ($62 \pm 23\%$) of air masses originating from the
194 Antarctic plateau reaching DDU (Fig. 4). The export of inland air masses towards the coastal
195 regions is not uniform across Antarctica and is concentrated in a few locations – “confluence
196 zones” – such as the Amery Ice Shelf region, the area near Adélie Land at 142° , the broad
197 region upslope from the Ross Ice Shelf, and the eastern side of the Antarctic Peninsula at \sim
198 60°W (Fig. 1) (Parish and Bromwich, 1987, 2007). Given its geographic location, DDU in
199 Adélie Land lies close to a confluence zone explaining the extent of the transport of air
200 masses from the Antarctic plateau. Conversely, several studies showed that stations such as
201 NM and HA are not significantly impacted by air masses originating from the Antarctic
202 plateau (Helmig et al., 2007; Legrand et al., 2016b), consistently explaining why Hg(0)
203 concentrations did not decrease at NM and TR throughout winter (Ebinghaus et al., 2002;
204 Pfaffhuber et al., 2012).

205 Despite the overall decreasing trend in winter, Hg(0) concentrations sporadically exhibited
206 abrupt increases when warm air masses from lower latitudes reached DDU. As illustrated by
207 Fig. 5, Hg(0) concentration for example increased from 0.72 (8 June 2012) to 1.10 ng m^{-3} (14
208 June 2012) with increasing temperature, and a significant positive correlation was found
209 between the two parameters ($r = 0.88$, p value < 0.0001 , Spearman test). This result is
210 supported by an enhanced fraction of oceanic air masses reaching DDU at that time according
211 to the HYSPLIT model simulations (Fig. 5d). Consistently, aerosol data gained in the
212 framework of the French environmental observation service CESOA ([http://www-
214 lgge.obs.ujf-grenoble.fr/CESOA/spip.php?rubrique3](http://www-
213 lgge.obs.ujf-grenoble.fr/CESOA/spip.php?rubrique3)) dedicated to the study of the sulfur
215 cycle at middle and high southern latitudes indicate a mean sodium concentration of 450 ng
216 m^{-3} between 10 and 14 June 2012 (not shown) instead of $112 \pm 62 \text{ ng m}^{-3}$ over the other days
217 of this month. It can be noted that the mean Hg(0) concentration in June 2012 was 0.95 ± 0.04
 ng m^{-3} at TR (Slemr et al., 2015), and $1.02 \pm 0.04 \text{ ng m}^{-3}$ on Amsterdam Island ($37^\circ 48'\text{S}$,

218 77°34'E, Angot et al., 2014). These values are consistent with the increase seen at DDU in air
219 masses arriving from lower latitudes.

220 **3.1.2 The ice-covered ocean as a sink for Hg(0) in spring**

221 First discovered in the Arctic in 1995 (Schroeder et al., 1998), Atmospheric Mercury
222 Depletion Events (AMDEs) have been subsequently observed after polar sunrise (mainly
223 from early September to the end of October) at coastal or near-coastal Antarctic stations at
224 NM (Ebinghaus et al., 2002), TNB (Sprovieri et al., 2002), MM (Brooks et al., 2008b), and
225 TR (Pfaffhuber et al., 2012). These events, characterized by abrupt decreases of Hg(0)
226 concentrations below 1.00 ng m⁻³ in the Arctic and 0.60 ng m⁻³ in Antarctica (Pfaffhuber et
227 al., 2012), result from the oxidation of Hg(0) by reactive bromine species (e.g., Schroeder et
228 al., 1998; Lu et al., 2001; Brooks et al., 2006; Sommar et al., 2007). At DDU, Hg(0) data
229 covering the spring time period are scarce (Fig. 2) and we can just emphasize that the absence
230 of Hg(0) drops in October 2012 tends to suggest that AMDEs, if exist, are not very frequent at
231 DDU. Ozone Depletion Events (ODEs) are found to be less frequent and far less pronounced
232 at DDU compared to other coastal stations such as NM and HA (Legrand et al., 2009;
233 Legrand et al., 2016b). Based on the oxygen and nitrogen isotope composition of airborne
234 nitrate at DDU, Savarino et al. (2007) concluded to an absence of significant implication of
235 BrO in the formation of nitric acid at this site, contrarily to what is usually observed in the
236 Arctic where high levels of BrO are measured at polar sunrise (Morin et al., 2008). All these
237 observations are consistent with a less efficient bromine chemistry in East compared to West
238 Antarctica due to a less sea-ice coverage, as also supported by GOME-2 satellite observations
239 of the tropospheric BrO column (Theys et al., 2011; Legrand et al., 2016a). Additionally, air
240 masses originating from the Antarctic plateau prevailed (62 ± 23 %, Fig. 4) in spring at DDU
241 according to the HYSPLIT model simulations. This can also explain, to some extent, the lack
242 of AMDE-observations at DDU.

243 Despite the absence of large AMDEs at DDU, springtime oceanic air masses were associated
244 with low Hg(0) concentrations (0.71 ± 0.11 ng m⁻³, see Fig. 3b). A slight but significant
245 negative correlation was found between Hg(0) concentrations in spring and the daily-averaged
246 percentage of oceanic air masses reaching DDU ($r = -0.38$, p value = 0.01, Spearman test)
247 while a significant positive correlation was observed between springtime Hg(0)
248 concentrations and O₃ mixing ratios in these oceanic air masses (r up to 0.65, p value <
249 0.0001, Spearman test). Therefore, though being not as pronounced as AMDEs observed at

250 other coastal stations, we cannot rule out that the rather low background Hg(0) levels
251 observed in spring at DDU are due to a weak effect of the bromine chemistry.

252 **3.2 High variability in Hg(0) concentrations in summer**

253 Hg(0) concentrations were highly variable during the sunlit period as compared to wintertime
254 (Fig. 2). Fig. 6 displays processes that may govern the atmospheric mercury budget at DDU in
255 summer, as discussed in the following sub-sections.

256 **3.2.1 Diurnal cycle of Hg(0) in ambient air**

257 Fig. 7 displays the monthly mean diurnal cycle of Hg(0) concentrations at DDU. Undetected
258 from March to October, a diurnal cycle characterized by a noon maximum was observed in
259 summer (November to February). Interestingly, Pfaffhuber et al. (2012) did not observe any
260 diurnal variation in Hg(0) concentrations at TR and there is no mention of a daily cycle at
261 NM, TNB, and MM (Ebinghaus et al., 2002; Temme et al., 2003; Sprovieri et al., 2002;
262 Brooks et al., 2008b).

263 Hg(0) concentrations at DDU were sorted according to wind speed and direction. With north
264 at 0°, oceanic winds ranged from 270 to 110°E, coastal winds from 110 to 130°E, katabatic
265 winds from 160 to 180°E, and continental winds from 130 to 160°E and from 180 to 270°E.
266 Summertime Hg(0) concentrations exhibited a diurnal cycle regardless of wind speed and
267 direction (Fig. 8). This result indicates that the observed diurnal cycle involves a local source
268 of Hg(0) around midday which is, moreover, specific to DDU since the diurnal cycle is not
269 observed at other coastal stations.

270 **3.2.1.1 Role of penguin emissions**

271 Large colonies of Adélie penguins nest on islands around DDU from the end of October to
272 late February, with a total population estimated at 60 000 individuals (Micol and Jouventin,
273 2001). Several studies highlighted that the presence of these large colonies at DDU in summer
274 significantly disturbs the atmospheric cycle of several species including ammonium and
275 oxalate (Legrand et al., 1998), carboxylic acids and other oxygenated volatile organic
276 compounds (Legrand et al., 2012), and HCHO (Preunkert et al., 2013). In a study
277 investigating sediment profiles excavated from ponds and catchments near penguin colonies
278 in the Ross Sea region, Nie et al. (2012) measured high mercury content in penguin excreta
279 (guano). Similarly, elevated total mercury concentrations were measured in ornithogenic soils
280 (i.e., formed by accumulation of guano) of the Fildes and Ardley peninsulas of King George

281 Island (De Andrade et al., 2012). When soil temperature rises above freezing in summer at
282 DDU, oxalate is produced together with ammonium following the bacterial decomposition of
283 uric acid in ornithogenic soils (Legrand et al., 1998 and references therein). Dicarboxylic
284 acids such as oxalic acid were shown to promote the light-driven reduction of Hg(II) species
285 in aqueous systems and ice (Gårdfeldt and Jonsson, 2003; Si and Ariya, 2008; Bartels-
286 Rausch et al., 2011). Emissions of Hg(0) from snow-covered ornithogenic soils are expected
287 to peak early and late summer – following the reduction of Hg(II) species in the upper layers
288 of the snowpack –, as also seen in the oxalate concentrations at DDU (Legrand et al., 1998).
289 Furthermore the rise of temperature at noon would strengthen Hg(0) emissions from
290 ornithogenic soils, possibly contributing to the observed diurnal cycle from November to
291 February.

292 **3.2.1.2 Possible role of the “sea breeze”**

293 In summer, the surface wind direction sometimes changes from 120-160°E to North as
294 temperature rises over midday (Pettré et al., 1993; Gallée and Pettré, 1998), giving birth to an
295 apparent sea breeze. This phenomenon usually lasts half a day or less and air masses cannot
296 be referred to as oceanic (see section 2.2.3). Legrand et al. (2001) and Legrand et al. (2016b)
297 observed increasing atmospheric dimethylsulfide (DMS) and chloride concentrations,
298 respectively, during sea breeze events. However, our results indicate that Hg(0)
299 concentrations did not tend to increase systematically with the occurrence of a sea breeze
300 (e.g., Fig. 9).

301 **3.2.1.3 Role of snowpack emissions**

302 Angot et al. (2016) reported a daily cycle in summer at DC with maximal Hg(0)
303 concentrations around midday. This daily cycle atop the East Antarctic ice sheet was
304 attributed to: i) an intense oxidation of Hg(0) in the atmospheric boundary layer due to the
305 high level of oxidants present there (Davis et al., 2001; Grannas et al., 2007; Eisele et al.,
306 2008; Kukui et al., 2014), ii) Hg(II) dry deposition onto the snowpack, and iii) increased
307 emission of Hg(0) from the snowpack around midday as a response to daytime heating
308 following photoreduction of Hg(II) in the upper layers of the snowpack. Even if DDU is
309 located on snow free bedrock for most of the summer season, the same mechanism could
310 apply since the station is surrounded by vast snow-covered areas. However, such a dynamic
311 cycle of deposition/reemission at the air/snow interface requires the existence of a

312 summertime atmospheric reservoir of Hg(II) species nearby DDU. This question is addressed
313 in the following sub-section.

314 **3.2.2 Transport of reactive air masses from the Antarctic plateau**

315 Several previous studies pointed out that the major oxidants present in the summer
316 atmospheric boundary layer at coastal Antarctic sites differ in nature from site to site:
317 halogens chemistry prevails in the West, OH/NO_x chemistry in the East (Legrand et al., 2009;
318 Grilli et al., 2013). Measurements made at HA in summer indicate a BrO mixing ratio of 3
319 pptv (Saiz-Lopez et al., 2007), a NO₂ mixing ratio of about 5 pptv (Bauguitte et al., 2012),
320 and a 24 h average value of 3.9×10^5 radicals cm⁻³ for OH (Bloss et al., 2007). Conversely,
321 BrO levels are at least lower by a factor of two at DDU (Legrand et al., 2016a) and Grilli et al.
322 (2013) reported a daily mean of 20 pptv for NO₂ in summer at DDU while Kukui et al. (2012)
323 reported a 24 h average value of 2.1×10^6 radicals cm⁻³ for OH. Large OH/NO_x concentrations
324 at DDU compared to HA were attributed to the arrival of air masses originating from the
325 Antarctic plateau where the OH/NO_x chemistry is very efficient (Legrand et al., 2009; Kukui
326 et al., 2012).

327 Goodsite et al. (2004) and Wang et al. (2014) suggested a two-step oxidation mechanism for
328 Hg(0), favored at cold temperatures. The initial recombination of Hg(0) and Br is followed by
329 the addition of a second radical (e.g., I, Cl, BrO, ClO, OH, NO₂, or HO₂) in competition with
330 the thermal dissociation of the HgBr intermediate. Using the rate constants calculated by
331 Wang et al. (2014) for the reactions of BrO, NO₂, and OH with the HgBr intermediate, we
332 found that BrO is the most efficient oxidant of HgBr at HA (lifetime of 1.9 min against 2.2
333 min with NO₂ and 11 days with OH). At DDU the situation is reversed with a lifetime of the
334 HgBr intermediate of 0.5 min with NO₂, 3.9 min with BrO (assuming the presence of 1.5 pptv
335 of BrO in summer at DDU (Legrand et al., 2016a)), and 2 hours with OH. These results
336 suggest that the formation of Hg(II) species at DDU could be promoted by oxidants
337 transported from the Antarctic plateau towards the coast.

338 In addition to oxidants, inland air masses may transport mercury species. Low Hg(0)
339 concentrations (0.76 ± 0.30 ng m⁻³) at DDU were associated with transport from the Antarctic
340 plateau in summer (November to February, see Fig. 3b). A significant negative correlation
341 was found in summer between Hg(0) concentrations and the daily-averaged percentage of air
342 masses originating from the Antarctic plateau ($r = -0.49$, p value < 0.0001, Spearman test).
343 Brooks et al. (2008a) reported elevated concentrations of oxidized mercury species at SP in

344 summer ($0.10 - 1.00 \text{ ng m}^{-3}$). Similarly, Angot et al. (2016) observed low Hg(0)
345 concentrations at the same period of the year at DC ($0.69 \pm 0.35 \text{ ng m}^{-3}$, i.e., $\sim 25\%$ lower
346 than at NM, TNB and MM). Angot et al. (2016) also reported the occurrence of multi-day to
347 weeklong Hg(0) depletion events (mean Hg(0) concentration $\sim 0.40 \text{ ng m}^{-3}$) likely due to a
348 stagnation of air masses above the plateau triggering an accumulation of oxidants within the
349 shallow boundary layer. These observations indicate that inland air masses reaching DDU in
350 summer are depleted in Hg(0) and enriched in Hg(II).

351 *Transect from central to coastal Antarctica*

352 The Hg_{tot} concentration of snow samples collected in summer 2009 between DC and DDU
353 (see section 2.2.2) ranged from 4.2 to 194.4 ng L^{-1} (Fig. 10). The closest sample from DC
354 exhibited a Hg_{tot} concentration of $60.3 \pm 8.1 \text{ ng L}^{-1}$ ($n = 3$), in very good agreement with
355 concentrations found in surface snow samples collected in summer at DC (up to $73.8 \pm 0.9 \text{ ng}$
356 L^{-1} , Angot et al., 2016). As illustrated by Fig. 10, Hg_{tot} concentrations increased between 600-
357 800 km and 1000-1100 km from DC in areas characterized by steeper slopes and higher snow
358 accumulation values. Several studies reported a gradual increase in snow accumulation from
359 DC toward the coast (Magand et al., 2007; Verfaillie et al., 2012; Favier et al., 2013), in
360 good agreement with a gradual increase in humidity (Bromwich et al., 2004). These results
361 suggest that the wet deposition of Hg(II) species was enhanced near the coast, resulting in
362 elevated Hg_{tot} concentrations in surface snow samples. Additionally, the presence of halides
363 such as chloride in snow can reduce the reduction rate of deposited Hg(II) species by
364 competing with the complexation of Hg(II) with dicarboxylic acids (Si and Ariya, 2008)
365 resulting in higher Hg_{tot} concentrations in coastal snowpacks (Steffen et al., 2014). It is worth
366 noting that the Hg_{tot} concentrations between DC and DDU were higher than the values
367 measured in summer along other expedition routes in East Antarctica. Han et al. (2011)
368 measured very low Hg_{tot} concentrations ($< 0.4 - 10.8 \text{ pg g}^{-1}$) along a $\sim 1500 \text{ km}$ transect in
369 east Queen Maud Land, and Hg_{tot} concentrations ranged from 0.2 to 8.3 ng L^{-1} along a
370 transect from ZG to DA (Fig. 1) (Li et al., 2014). Unfortunately none of the samples collected
371 during these two traverses were truly coastal – the most seaward samples were collected at
372 altitudes of 948 and 622 m, respectively – preventing a direct comparison with the
373 concentration measured near DDU. The mean Hg_{tot} concentration of $67 \pm 21 \text{ ng L}^{-1}$ reported
374 by Brooks et al. (2008b) at MM is the only truly coastal value available in Antarctica and is
375 lower than the value reported here near DDU.

376 The advection of inland air masses enriched in both oxidants and Hg(II) likely results in the
377 build-up of an atmospheric reservoir of Hg(II) species at DDU – as confirmed by elevated
378 Hg_{tot} concentrations in surface snow samples –, confirming the hypothesis of a dynamic cycle
379 of deposition/reemission at the air/snow interface.

380 **3.2.3 The ocean as a source of Hg(0)**

381 DDU is located on a small island with open ocean immediately around from December to
382 February. It should be noted that during summers 2011/2012, 2012/2013, and 2013/2014,
383 areas of open waters were observed but with a significant unusual large amount of sea ice.
384 Sea ice maps can be obtained from [http://www.iup.uni-](http://www.iup.uni-bremen.de:8084/amsr2data/asi_daygrid_swath/s6250/)
385 [bremen.de:8084/amsr2data/asi_daygrid_swath/s6250/](http://www.iup.uni-bremen.de:8084/amsr2data/asi_daygrid_swath/s6250/) (Spren et al., 2008).

386 According to Fig. 3b, Hg(0) concentrations in oceanic air masses were elevated from
387 December to February ($1.04 \pm 0.29 \text{ ng m}^{-3}$), and a significant positive correlation was found
388 between Hg(0) concentrations and the daily-averaged percentage of oceanic air masses in
389 summer ($r = 0.50$, p value < 0.0001 , Spearman test). While in winter the ice cover limited
390 mercury exchange at the air/sea interface (Andersson et al., 2008) leading to the build-up of
391 mercury-enriched waters, large emissions of Hg(0) from the ocean likely occurred in summer.
392 According to Cossa et al. (2011), total mercury concentrations can be one order of magnitude
393 higher in under-ice seawater than those measured in open ocean waters. The authors attributed
394 this build-up of mercury-enriched surface waters to the massive algal production at basal sea
395 ice in spring/summer triggering a large production of Hg(0), and to the mercury enrichment in
396 brine during the formation of sea ice. Elevated Hg(0) concentrations in oceanic air masses are
397 consistent with observations in the Arctic where Hg(0) concentrations in ambient air peak in
398 summer due to oceanic evasion and snowmelt revolatilization (Dastoor and Durnford, 2014).
399 Additionally, evasion from meltwater ponds formed on the remaining sea ice and observed
400 around the station may contribute to the increase in Hg(0) concentrations (Aspmo et al., 2006;
401 Durnford and Dastoor, 2011).

402

403 **4 Implications**

404 **4.1 For coastal Antarctic ecosystems**

405 The reactivity of atmospheric mercury is unexpectedly significant in summer on the Antarctic
406 plateau as evidenced by elevated Hg(II) and low Hg(0) concentrations (Brooks et al., 2008a;

407 Dommergue et al., 2012; Angot et al., 2016). This study shows that katabatic/continental
408 winds can transport this inland atmospheric reservoir toward the coastal margins where Hg(II)
409 species tend to deposit due to increasing wet deposition (Fig. 10). However, the
410 postdeposition dynamics of mercury and its ultimate fate in ecosystems remain unknown.
411 Bargagli et al. (1993) and Bargagli et al. (2005) showed evidence of enhanced
412 bioaccumulation of mercury in soils, mosses, and lichens collected in ice-free areas around
413 the Nansen Ice Sheet (Victoria Land, upslope from the Ross Ice Shelf), suggesting an
414 enhanced deposition of mercury species. Interestingly, four large glaciers join in the Nansen
415 Ice Sheet region and channel the downward flow of air masses from the Antarctic plateau
416 toward Terra Nova Bay, generating intense katabatic winds. The monthly mean wind speed is
417 about 16 m s^{-1} in this area (Bromwich, 1989). Along with an enhanced deposition of mercury
418 during AMDEs, the wind might as well be responsible for the advection of inland air masses
419 enriched in Hg(II) species as observed in our case study. As already pointed out by Bargagli
420 et al. (2005), coastal Antarctic ecosystems may become a sink for mercury, especially in view
421 of increasing anthropogenic emissions of mercury in Asia (Streets et al., 2009).

422 **4.2 For the cycle of atmospheric mercury in high southern latitudes**

423 The influence of the Antarctic continent on the global geochemical cycle of mercury remains
424 unclear (Dommergue et al., 2010). This study shows that the reactivity observed on the
425 Antarctic plateau (Brooks et al., 2008a; Dommergue et al., 2012; Angot et al., 2016)
426 influences the cycle of atmospheric mercury at a continental scale, especially downstream of
427 the main topographic confluence zones. The question is whether the katabatic airflow
428 propagation over the ocean is important. According to Mather and Miller (1967), the katabatic
429 flow draining from the Antarctic plateau merges with the coastal polar easterlies under the
430 action of the Coriolis force. The near-surface flow takes the form of an anticyclonic vortex
431 (King and Turner, 1997), limiting the propagation of katabatic flows over the ocean.

432

433 **5 Conclusion**

434 We presented here a 3.5-year record of Hg(0) concentrations at DDU, first multi-year record
435 on the East Antarctic coast. Our observations reveal a number of differences with other coastal
436 or near coastal Antarctic records. In winter, observations showed a gradual 20% decrease in
437 Hg(0) concentrations from May to August, a trend never observed at other coastal sites. This
438 is interpreted as a result of reactions occurring within the shallow boundary layer on the

439 Antarctic plateau, subsequently efficiently transported at that site by katabatic winds. In
440 summer, the advection of inland air masses enriched in oxidants and Hg(II) species likely
441 results in the build-up of an atmospheric reservoir of Hg(II) species at DDU, at least partly
442 explaining the elevated (up to 194.4 ng L⁻¹) Hg_{tot} concentrations measured in surface snow
443 samples near the station during a traverse between DC and DDU. Additionally, Hg(0)
444 concentrations in ambient air exhibited a diurnal cycle in summer at DDU – phenomenon
445 never observed at other coastal Antarctic stations. Several processes may contribute to this
446 diurnal cycle, including a local chemical exchange at the air/snow interface in the presence of
447 elevated levels of Hg(II) species in ambient air, and emissions from ornithogenic soils present
448 at the site. Our data also highlight the fact that the Austral Ocean may be a net source for
449 mercury in the summer. Even though AMDEs are likely very rare at DDU compared to other
450 coastal stations, we cannot exclude that the sea-ice present offshore DDU at the end of winter
451 influenced springtime Hg(0) levels. Finally, having shown that the reactivity observed on the
452 Antarctic plateau influences the cycle of atmospheric mercury on the East Antarctic coast, this
453 study raises concern for coastal Antarctic ecosystems there.

454

455 **Acknowledgements**

456 We thank the overwintering crew: S. Aguado, D. Buiron, N. Coillard, G. Dufresnes, J.
457 Guilhermet, B. Jourdain, B. Laulier, S. Oros, and A. Thollot. We also gratefully acknowledge
458 M. Barret for the development of a QA/QC software program, Météo France for the
459 meteorological data, and Susanne Preunkert who helped to validate contamination-free ozone
460 data. This work contributed to the EU-FP7 project Global Mercury Observation System
461 (GMOS – www.gmos.eu) and has been supported by a grant from Labex OSUG@2020
462 (Investissements d'avenir – ANR10 LABX56), and the Institut Universitaire de France.
463 Logistical and financial support was provided by the French Polar Institute IPEV (Program
464 1028, GMOstral).

References

- Andersson, M. E. S., J., Gårdfeldt, K., and Linfquist, O.: Enhanced concentrations of dissolved gaseous mercury in the surface waters of the Arctic Ocean, *Marine Chemistry*, 110, 190-194, 2008.
- Angot, H., Barret, M., Magand, O., Ramonet, M., and Dommergue, A.: A 2-year record of atmospheric mercury species at a background Southern Hemisphere station on Amsterdam Island, *Atmospheric Chemistry and Physics* 14, 11461-11473, 2014.
- Angot, H., Magand, O., Helmig, D., Ricaud, P., Quennehen, B., Gallée, H., Del Guasta, M., Sprovieri, F., Pirrone, N., Savarino, J., and Dommergue, A.: New insights into the atmospheric mercury cycling in Central Antarctica and implications at a continental scale, *Atmospheric Chemistry and Physics Discussions*, 10.5194/acp-2016-144, in review, 2016.
- Aspmo, K., Temme, C., Berg, T., Ferrari, C., Gauchard, P.-A., Fain, X., and Wibetoe, G.: Mercury in the atmosphere, snow and melt water ponds in the north atlantic ocean during Arctic summer, *Environmental Science and Technology*, 40, 4083-4089, 2006.
- Bargagli, R., Battisti, E., Focardi, S., and Formichi, P.: Preliminary data on environmental distribution of mercury in northern Victoria Land, Antarctica, *Antarctic Science*, 5, 3-8, 1993.
- Bargagli, R., Agnorelli, C., Borghini, F., and Monaci, F.: Enhanced deposition and bioaccumulation of mercury in antarctic terrestrial ecosystems facing a coastal polynya, *Environmental Science and Technology*, 39, 8150-8155, 2005.
- Bartels-Rausch, T., Krysztofiak, G., Bernhard, A., Schläppi, M., Schwikowski, M., and Ammann, M.: Photoinduced reduction of divalent mercury in ice by organic matter, *Chemosphere*, 82, 199-203, 2011.
- Bauguitte, S. J.-B., Bloss, W. J., Evans, M. J., Salmon, R. A., Anderson, P. S., Jones, A. E., Lee, J. D., Saiz-Lopez, A., Roscoe, H. K., Wolff, E. W., and Plane, J. M. C.: Summertime NO_x measurements during the CHABLIS campaign: can source and sink estimates unravel observed diurnal cycles?, *Atmospheric Chemistry and Physics*, 12, 989-1002, 2012.
- Bloss, W. J., Lee, J. D., Heard, D. E., Salmon, R. A., Bauguitte, S. J.-B., Roscoe, H. K., and Jones, A. E.: Observations of OH and HO₂ radicals in coastal Antarctica, *Atmospheric Chemistry and Physics*, 7, 4171-4185, 2007.
- Bromwich, D., Guo, Z., Bai, L., and Chen, Q.: Modeled antarctic precipitation. Part I: spatial and temporal variability., *J. Climate*, 17, 427-447, 2004.
- Bromwich, D. H.: An extraordinary katabatic wind regime at Terra Nova Bay, Antarctica, *Monthly Weather Review*, 117, 688-695, 1989.
- Brooks, S., Saiz-Lopez, A., Skov, H., Lindberg, S. E., Plane, J. M. C., and Goodsite, M. E.: The mass balance of mercury in the springtime arctic environment, *Geophysical research letters*, doi: 10.1029/2005GL025525, 2006.
- Brooks, S. B., Arimoto, R., Lindberg, S. E., and Southworth, G.: Antarctic polar plateau snow surface conversion of deposited oxidized mercury to gaseous elemental mercury with fractional long-term burial, *Atmospheric Environment*, 42, 2877-2884, 2008a.
- Brooks, S. B., Lindberg, S. E., Southworth, G., and Arimoto, R.: Springtime atmospheric mercury speciation in the McMurdo, Antarctica coastal region, *Atmospheric Environment*, 42, 2885-2893, 2008b.

- Chen, D., Hale, R. C., La Guardia, M. J., Luellen, D., Kim, S., and Geisz, H. N.: Hexabromocyclododecane flame retardant in Antarctica: research station as sources, *Environmental Pollution*, 206, 611-618, 2015.
- Cossa, D., Heimbürger, L.-E., Lannuzel, D., Rintoul, S. R., Butler, E. C. V., Bowie, A. R., Averty, B., Watson, R. J., and Remenyi, T.: Mercury in the Southern Ocean, *Geochimica et Cosmochimica Acta*, 75, 4037-4052, 2011.
- D'Amore, F., Bencardino, M., Cinnirella, S., Sprovieri, F., and Pirrone, N.: Data quality through a web-based QA/QC system: implementation for atmospheric mercury data from the Global Mercury Observation System, *Environmental Science: Processes & Impacts*, 17, 1482-1491, 2015.
- Dastoor, A. P., and Durnford, D. A.: Arctic ocean: is it a sink or a source of atmospheric mercury?, *Environmental Science and Technology*, 48, 1707-1717, 2014.
- Davis, D., Nowak, J. B., Chen, G., Buhr, M., Arimoto, R., Hogan, A., Eisele, F., Mauldin, L., Tanner, D., Shetter, R., Lefer, B., and McMurry, P.: Unexpected high levels of NO observed at South Pole, *Geophysical research letters*, 28, 3625-3628, 2001.
- De Andrade, R. P., Michel, R. F. M., Schaefer, C. E. G. R., Simas, F. N. B., and Windmüller, C. C.: Hg distribution and speciation in Antarctic soils of the Fildes and Ardley peninsulas, King George Island, *Antarctic Science*, 24, 395-407, 2012.
- Dommergue, A., Sprovieri, F., Pirrone, N., Ebinghaus, R., Brooks, S., Courteaud, J., and Ferrari, C. P.: Overview of mercury measurements in the antarctic troposphere, *Atmospheric Chemistry and Physics*, 10, 3309-3319, 2010.
- Dommergue, A., Barret, M., Courteaud, J., Cristofanelli, P., Ferrari, C. P., and Gallée, H.: Dynamic recycling of gaseous elemental mercury in the boundary layer of the antarctic plateau, *Atmospheric Chemistry and Physics*, 12, 11027-11036, 2012.
- Draxler, R. R., and Rolph, G. D.: HYSPLIT (HYbrid Single-Particle Lagrangian Integrated Trajectory) Model access via NOAA ARL READY Website (<http://www.arl.noaa.gov/HYSPLIT.php>), last access: 24 October 2015. NOAA Air Resources Laboratory, College Park, MD. , 2013.
- Dumarey, R., Temmerman, E., Dams, R., and Hoste, J.: The accuracy of the vapour injection calibration method for the determination of mercury by amalgamation/cold vapour atomic spectrometry, *Analytica Chimica Acta*, 170, 337-340, 1985.
- Durnford, D., and Dastoor, A.: The behavior of mercury in the cryosphere: a review of what we know from observations, *Journal of geophysical research*, 116, doi:10.1029/2010JD014809, 2011.
- Ebinghaus, R., Kock, H. H., Temme, C., Einax, J. W., Löwe, A. G., Richter, A., Burrows, J. P., and Schroeder, W. H.: Antarctic springtime depletion of atmospheric mercury, *Environmental Science and Technology*, 36, 1238-1244, 2002.
- Eisele, F., Davis, D. D., Helmig, D., Oltmans, S. J., Neff, W., Huey, G., Tanner, D., Chen, G., Crawford, J. H., Arimoto, R., Buhr, M., Mauldin, L., Hutterli, M., Dibb, J., Blake, D., Brooks, S. B., Johnson, B., Roberts, J. M., Wang, Y., Tan, D., and Flocke, F.: Antarctic tropospheric chemistry (ANTCI) 2003 overview, *Atmospheric Environment*, 2008, 2749-2761, 2008.
- Favier, V., Agosta, C., Parouty, S., Durand, G., Delaygue, G., Gallée, H., Drouet, A.-S., Trouvilliez, A., and Krinner, G.: An updated and quality controlled surface mass balance dataset for Antarctica, *The Cryosphere*, 7, 583-597, 2013.

- Gallée, H., and Pettré, P.: Dynamical constraints on katabatic wind cessation in Adélie Land, Antarctica, *Journal of the atmospheric sciences*, 55, 1755-1770, 1998.
- Gårdfeldt, K., and Jonsson, M.: Is biomolecular reduction of Hg(II) complexes possible in aqueous systems of environmental importance, *Journal of physical chemistry A*, 107, 4478-4482, 2003.
- Goodsite, M. E., Plane, J. M. C., and Skov, H.: A theoretical study of the oxidation of Hg⁰ to HgBr₂ in the troposphere, *Environmental Science and Technology*, 38, 1772-1776, 2004.
- Grannas, A. M., Jones, A. E., Dibb, J., Ammann, M., Anastasio, C., Beine, H. J., Bergin, M., Bottenheim, J., Boxe, C. S., Carver, G., Chen, G., Crawford, J. H., Domine, F., Frey, M. M., Guzman, M. I., Heard, D. E., Helmig, D., Hoffmann, M. R., Honrath, R. E., Huey, L. G., Hutterli, M., Jacobi, H.-W., Klan, P., Lefer, B., McConnell, J. R., Plane, J. M. C., Sander, R., Savarino, J., Shepson, P. B., Simpson, W. R., Sodeau, J., Von Glasow, R., Weller, R., Wolff, E. W., and Zhu, T.: An overview of snow photochemistry: evidence, mechanisms and impacts, *Atmospheric Chemistry and Physics*, 7, 4329-4373, 2007.
- Grilli, R., Legrand, M., Kukui, A., Méjean, G., Preunkert, S., and Romanini, D.: First investigations of IO, BrO, and NO₂ summer atmospheric levels at a coastal East Antarctic site using mode-locked cavity enhanced absorption spectroscopy, *Geophysical research letters*, 40, 791-796, 2013.
- Hale, R. C., Kim, S. L., Harvey, E., La Guardia, M. J., Mainor, T. M., Bush, E. O., and Jacobs, E. M.: Antarctic research bases: local sources of polybrominated diphenyl ether (PBDE) flame retardants, *Environmental Science and Technology*, 42, 1452-1457, 2008.
- Han, Y., Huh, Y., Hong, S., Hur, S. D., Motoyama, H., Fujita, S., Nakazawa, F., and Fukui, K.: Quantification of total mercury in Antarctic surface snow using ICP-SF-MS: spatial variation from the coast to Dome Fuji, *Bulletin of Korean Chemical Society*, 32, 4258-4264, 2011.
- Helmig, D., Oltmans, S. J., Carlson, D., Lamarque, J.-F., Jones, A., Labuschagne, C., Anlauf, K., and Hayden, K.: A review of surface ozone in the polar regions, *Atmospheric Environment*, 41, 5138-5161, 2007.
- Jaffe, D. A., Prestbo, E., Swartzendruber, P., Weiss-Penzias, P., Kato, S., Takami, A., Hatakeyama, S., and Kajii, Y.: Export of atmospheric mercury from Asia, *Atmospheric Environment*, 2005, 3029-3038, 2005.
- King, J. C., and Turner, J.: *Antarctic Meteorology and Climatology*, Cambridge University Press, 409 pp., 1997.
- König-Langlo, G., King, J. C., and Pettré, P.: Climatology of the three coastal Antarctic stations Dumont d'Urville, Neumayer, and Halley, *Journal of geophysical research*, 103, 10935-10946, 1998.
- Kukui, A., Legrand, M., Ancellet, G., Gros, V., Bekki, S., Sarda-Estève, R., Loisil, R., and Preunkert, S.: Measurements of OH and RO₂ radicals at the coastal Antarctic site of Dumont d'Urville (East Antarctica) in summer 2010-2011, *Journal of geophysical research*, 117, doi:10.1029/2012JD017614, 2012.
- Kukui, A., Legrand, M., Preunkert, S., Frey, M. M., Loisil, R., Gil Roca, J., Jourdain, B., King, M. D., France, J. L., and Ancellet, G.: Measurements of OH and RO₂ radicals at Dome C, East Antarctica, *Atmospheric Chemistry and Physics*, 14, 12373-12392, 2014.

- Legrand, M., Ducroz, F., Wagenbach, D., Mulvaney, R., and Hall, J.: Ammonium in coastal Antarctic aerosol and snow: role of polar ocean and penguin emissions, *Journal of geophysical research*, 103, 11043-11056, 1998.
- Legrand, M., Sciare, J., Jourdain, B., and Genthon, C.: Subdaily variations of atmospheric dimethylsulfide, dimethylsulfoxide, methanesulfonate, and non-sea-salt sulfate aerosols in the atmospheric boundary layer at Dumont d'Urville (coastal Antarctica) during summer, *Journal of geophysical research*, 106, 14409-14422, 2001.
- Legrand, M., Preunkert, S., Jourdain, B., Gallée, H., Goutail, F., Weller, R., and Savarino, J.: Year-round record of surface ozone at coastal (Dumont d'Urville) and inland (Concordia) sites in east antarctica, *Journal of geophysical research*, 114, doi:10.1029/2008JD011667, 2009.
- Legrand, M., Gros, V., Preunkert, S., Sarda-Estève, R., Thierry, A.-M., Pépy, G., and Jourdain, B.: A reassessment of the budget of formic and acetic acids in the boundary layer at Dumont d'Urville (coastal Antarctica): the role of penguin emissions on the budget of several oxygenated volatile organic compounds, *Journal of geophysical research*, 117, doi: 10.1029/2011JD017102, 2012.
- Legrand, M., Yang, X., Preunkert, S., and Theys, N.: Year-round records of sea salt, gaseous, and particulate inorganic bromine in the atmospheric boundary layer at coastal (Dumont d'Urville) and central (Concordia) East Antarctic sites, *Journal of geophysical research: atmospheres*, 121, DOI: 10.1002/2015JD024066, 2016a.
- Legrand, M. P., S., Savarino, J., Frey, M. M., Kukui, A., Helmig, D., Jourdain, B., Jones, A., Weller, R., Brough, N., and Gallée, H.: Inter-annual variability of surface ozone at coastal (Dumont d'Urville, 2004-2014) and inland (Concordia, 2007-2014) sites in East Antarctica, *Atmospheric Chemistry and Physics*, doi:10.5194/acp-2016-95, in press, 2016b.
- Li, C., Kang, S., Shi, G., Huang, J., Ding, M., Zhang, Q., Zhang, L., Guo, J., Xiao, C., Hou, S., Sun, B., Qin, D., and Ren, J.: Spatial and temporal variations of total mercury in Antarctic snow along the transect from Zhongshan station to Dome A, *Tellus*, 66, <http://dx.doi.org/10.3402/tellusb.v66.25152>, 2014.
- Lin, C.-J., and Pehkonen, S. O.: The chemistry of atmospheric mercury: a review, *Atmospheric Environment*, 33, 2067-2079, 1999.
- Lindberg, S. E., and Stratton, W. J.: Atmospheric mercury speciation: concentrations and behavior of reactive gaseous mercury in ambient air, *Environmental Science and Technology*, 32, 49-57, 1998.
- Lindberg, S. E., Bullock, R., Ebinghaus, R., Engstrom, D., Feng, X., Fitzgerald, W. F., Pirrone, N., Prestbo, E., and Seigneur, C.: A synthesis of progress and uncertainties in attributing the sources of mercury in deposition, *Ambio*, 36, 19-32, 2007.
- Lindqvist, O., and Rodhe, H.: Atmospheric mercury - a review, *Tellus*, 37B, 136-159, 1985.
- Lu, J. Y., Schroeder, W. H., Barrie, L. A., Steffen, A., Welch, H. E., Martin, K., Lockhart, L., Hunt, R. V., Boila, G., and Richter, A.: Magnification of atmospheric mercury deposition to polar regions in springtime: the link to tropospheric ozone depletion chemistry, *Geophysical research letters*, 28, 3219-3222, 2001.
- Magand, O., Genthon, C., Fily, M., Krinner, G., Picard, G., Frezzotti, M., and Ekaykin, A.: An up-to-date quality-controlled surface mass balance data set for the 90°-180°E Antarctica sector and 1950-2005 period, *Journal of geophysical research*, 112, doi: 10.1029/2006JD007691, 2007.

- Mather, K. B., and Miller, G. S.: The problem of the katabatic winds on the coast of Terre Adélie, *Polar Record*, 13, 425-432, 1967.
- Micol, T., and Jouventin, P.: Long-term population trends in seven Antarctic seabirds at Pointe Géologie (Terre Adélie). Human impact compared with environmental change, *Polar Biology*, 24, 175-185, 2001.
- Morin, S., Savarino, J., Frey, M. M., Yan, N., Bekki, S., Bottenheim, J. W., and Martins, J. M. F.: tracing the origin and fate of NO_x in the Arctic atmosphere using stable isotopes *Science*, 322, doi: 10.1126/science.1161910, 2008.
- Munthe, J., Sprovieri, F., Horvat, M., and Ebinghaus, R.: SOPs and QA/QC protocols regarding measurements of TGM, GEM, RGM, TPM and mercury in precipitation in cooperation with WP3, WP4 and WP5. GMOS deliverable 6.1, CNR-IIA, IVL. <http://www.gmos.eu>, last access: 3 March 2014, 2011.
- Nie, Y., Liu, X., Sun, L., and Emslie, S. D.: Effect of penguin and seal excrement on mercury distribution in sediments from the Ross Sea region, East Antarctica, *Science of the Total Environment*, 433, 132-140, 2012.
- Parish, T. R., and Bromwich, D. H.: The surface windfield over the Antarctic ice sheets, *Nature*, 328, 51-54, 1987.
- Parish, T. R., and Bromwich, D. H.: Reexamination of the near-surface airflow over the Antarctic continent and implications on atmospheric circulations at high southern latitudes, *Monthly Weather Review*, 135, 1961-1973, 2007.
- Pettré, P., Payan, C., and Parish, T. R.: Interaction of katabatic flow with local thermal effects in a coastal region of Adelie Land, East Antarctica, *Journal of geophysical research*, 98, 10429-10440, 1993.
- Pfaffhuber, K. A., Berg, T., Hirdman, D., and Stohl, A.: Atmospheric mercury observations from Antarctica: seasonal variation and source and sink region calculations, *Atmospheric Chemistry and Physics*, 12, 3241-3251, 2012.
- Preunkert, S., Legrand, M., Pépy, G., Gallée, H., Jones, A., and Jourdain, B.: The atmospheric HCHO budget at Dumont d'Urville (East Antarctica): contribution of photochemical gas-phase production versus snow emissions, *Journal of geophysical research: atmospheres*, 118, 13319-13337, 2013.
- Saiz-Lopez, A., Mahajan, A. S., Salmon, R. A., Bauguitte, S. J.-B., Jones, A. E., Roscoe, H. K., and Plane, J. M. C.: Boundary layer halogens in coastal Antarctica, *Science*, 317, 348-351, 2007.
- Savarino, J., Kaiser, J., Morin, S., Sigman, D. M., and Thiemens, M. H.: Nitrogen and oxygen isotopic constraints on the origin of atmospheric nitrate in coastal Antarctica, *Atmospheric Chemistry and Physics*, 7, 1925-1945, 2007.
- Schroeder, W. H., Anlauf, K. G., Barrie, L. A., Lu, J. Y., Steffen, A., Schneeberger, D. R., and Berg, T.: Arctic springtime depletion of mercury, *Nature*, 394, 331-332, 1998.
- Schroeder, W. H., and Munthe, J.: Atmospheric mercury - an overview, *Atmospheric Environment*, 32, 809-822, 1998.
- Shirsat, S. V., and Graf, H. F.: An emission inventory of sulfur from anthropogenic sources in Antarctica, *Atmospheric Chemistry and Physics*, 9, 3397-3408, 2009.
- Si, L., and Ariya, P. A.: Reduction of oxidized mercury species by dicarboxylic acids (C₂-C₄): kinetic and product studies, *Environmental Science and Technology*, 42, 5150-5155, 2008.

Slemr, F., Angot, H., Dommergue, A., Magand, O., Barret, M., Weigelt, A., Ebinghaus, R., Brunke, E.-G., Pfaffhuber, K. A., Edwards, G., Howard, D., Powell, J., Keywood, M., and Wang, F.: Comparison of mercury concentrations measured at several sites in the Southern Hemisphere, *Atmospheric Chemistry and Physics*, 15, 3125-3133, 2015.

Sommar, J., Wängberg, I., Berg, T., Gårdfeldt, K., Munthe, J., Richter, A., Urba, A., Wittrock, F., and Schroeder, W. H.: Circumpolar transport and air-surface exchange of atmospheric mercury at Ny-Alesund (79°N), Svalbard, spring 2002, *Atmos. Chem. Phys.*, 7, 151-166, 10.5194/acp-7-151-2007, 2007.

Spren, G., Kaleschke, L., and Heygster, G.: Sea ice remote sensing using AMSR-E 89 GHz channels, *Journal of geophysical research*, 113, <http://dx.doi.org/10.1029/2005JC003384>, 2008.

Sprovieri, F., Pirrone, N., Hedgecock, I. M., Landis, M. S., and Stevens, R. K.: Intensive atmospheric mercury measurements at Terra Nova Bay in antarctica during November and December 2000, *Journal of geophysical research*, 107, 4722, 2002.

Steffen, A., Schroeder, W., Bottenheim, J., Narayan, J., and Fuentes, J. D.: Atmospheric mercury concentrations: measurements and profiles near snow and ice surfaces in the Canadian Arctic during Alert 2000, *Atmospheric Environment*, 36, 2653-2661, 2002.

Steffen, A., Douglas, T., Amyot, M., Ariya, P. A., Aspino, K., Berg, T., Bottenheim, J., Brooks, S., Cobbett, F., Dastoor, A., Dommergue, A., Ebinghaus, R., Ferrari, C., Gardfeldt, K., Goodsite, M. E., Lean, D., Poulain, A. J., Scherz, C., Skov, H., Sommar, J., and Temme, C.: A synthesis of atmospheric mercury depletion event chemistry in the atmosphere and snow, *Atmospheric Chemistry and Physics*, 8, 1445-1482, 2008.

Steffen, A., Scherz, T., Oslon, M., Gay, D. A., and Blanchard, P.: A comparison of data quality control protocols for atmospheric mercury speciation measurements, *Journal of Environmental Monitoring*, 14, 752-765, doi: 10.1039/c2em10735j, 2012.

Steffen, A., Lehnerr, I., Cole, A., Ariya, P. A., Dastoor, A., Durnford, D., Kirk, J., and Pilote, M.: Atmospheric mercury in the Canadian Arctic. Part I: A review of recent field measurements, *Science of the Total Environment*, <http://dx.doi.org/10.1016/j.scitotenv.2014.1010.1109>, 2014.

Stohl, A.: Computation, accuracy and application of trajectories - a review and bibliography, *Atmospheric Environment*, 32, 947-966, 1998.

Streets, D. G., Zhang, Q., and Wu, Y.: Projections of global mercury emissions in 2050, *Environmental Science and Technology*, 43, 2983-2988, 2009.

Tekran: Tekran 2537 mercury monitor detection limit. Summary of known estimates, Tekran Instruments Corp., Toronto, ON, Canada., 2011.

Temme, C., Einax, J. W., Ebinghaus, R., and Schroeder, W. H.: Measurements of atmospheric mercury species at a coastal site in the antarctic and over the atlantic ocean during polar summer, *Environmental Science and Technology*, 37, 22-31, 2003.

Theys, N., Van Roozendaal, M., Hendrick, F., Yang, X., De Smedt, I., Richter, A., Begoin, M., Errera, Q., Johnston, P. V., Kreher, K., and De Mazière, M.: Global observations of tropospheric BrO columns using GOME-2 satellite data, *Atmospheric Chemistry and Physics*, 11, 1791-1811, 2011.

Verfaillie, D., Fily, M., Le Meur, E., Magand, O., Jourdain, B., Arnaud, L., and Favier, V.: Snow accumulation variability derived from radar and firn core data along a 600 km transect in Adelie Land, East Antarctic plateau, *The Cryosphere*, 6, 1345-1358, 2012.

Wang, F., Saiz-Lopez, A., Mahajan, A. S., Gomez Martin, J. C., Armstrong, D., Lemes, M., Hay, T., and Prados-Roman, C.: Enhanced production of oxidised mercury over the tropical pacific ocean: a key missing oxidation pathway, *Atmospheric Chemistry and Physics*, 14, 1323-1335, 2014.

Yu, S., Mathur, R., Kang, D., Schere, K., and Tong, D.: A study of the ozone formation by ensemble back trajectory-process analysis using the Eta-CMAQ forecast model over the northeastern U.S. during the 2004 ICARTT period, *Atmospheric Environment*, 43, 355-363, 2009.

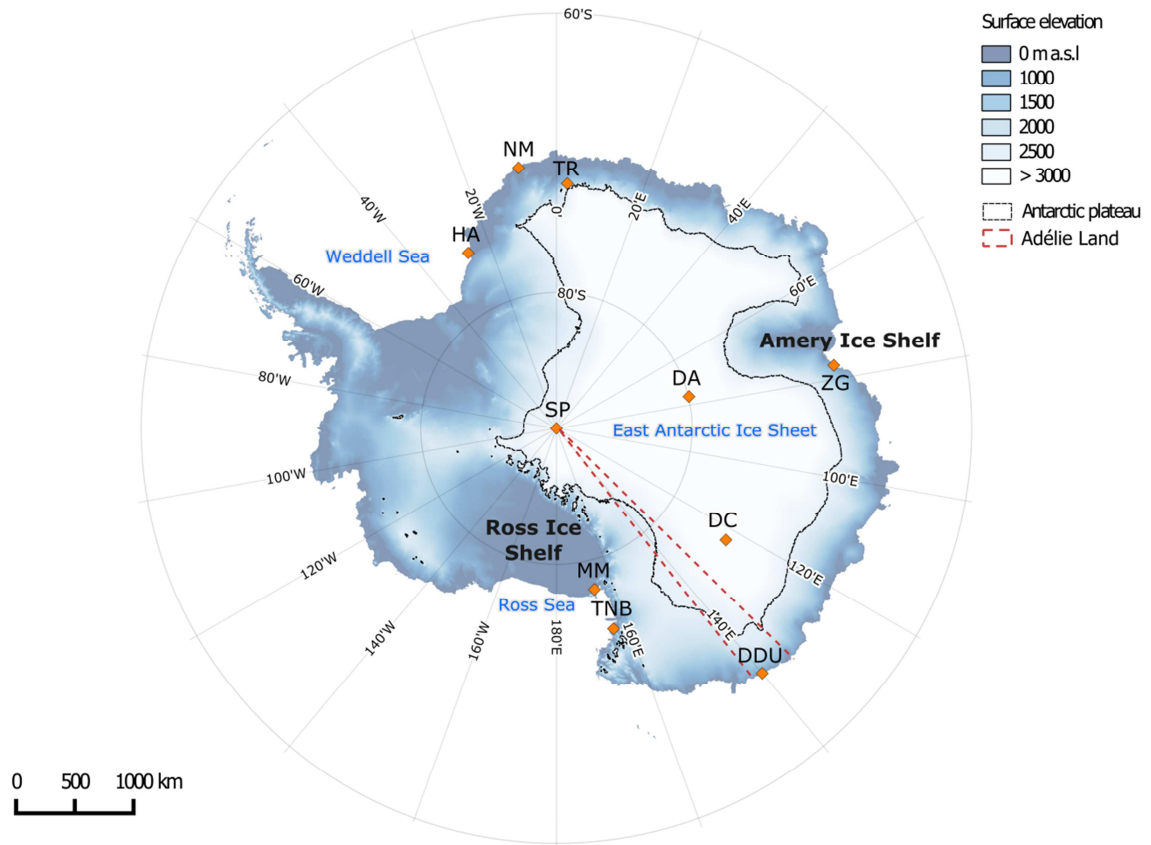


Figure 1: Map of Antarctica showing surface elevation (meters above sea level, m a.s.l) and the position of various stations: Halley (HA), Neumayer (NM), Troll (TR), Zhongshan Station (ZG), Dome A (DA), South Pole Station (SP), Concordia Station (DC), Dumont d'Urville (DDU), McMurdo (MM), and Terra Nova Bay (TNB). The black line delimits the high altitude plateau (> 2500 m a.s.l), and the red dotted line Adélie Land (from 136°E to 142°E).

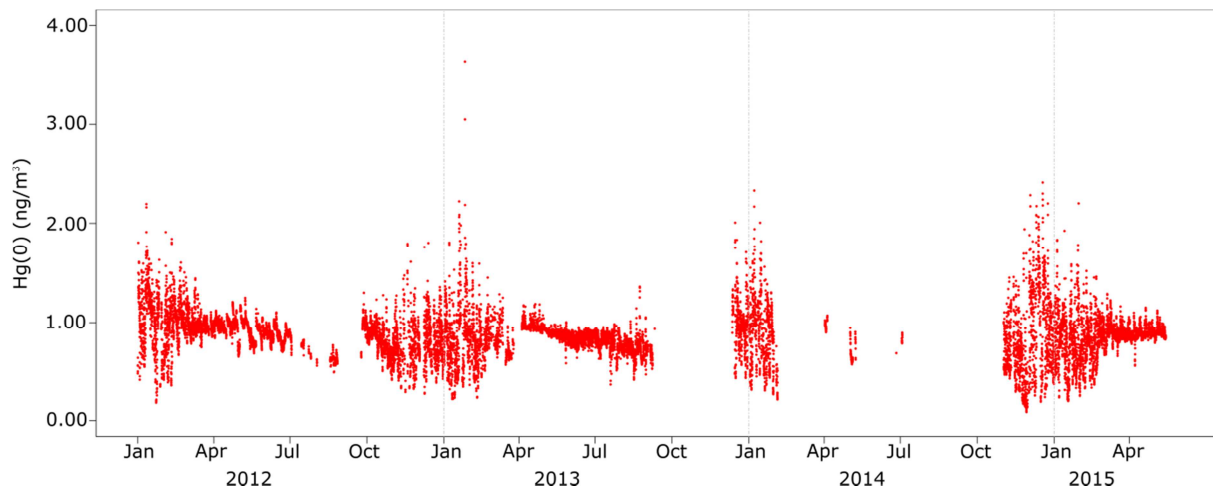


Figure 2: Hourly-averaged Hg(0) concentrations (ng/m^3) measured at DDU from January 2012 to May 2015. Missing data are due to instrument failure or QA/QC invalidation. Hg(0) concentrations were highly variable during the sunlit period as compared to wintertime (May-August) suggesting a photochemically-induced reactivity at this period of the year.

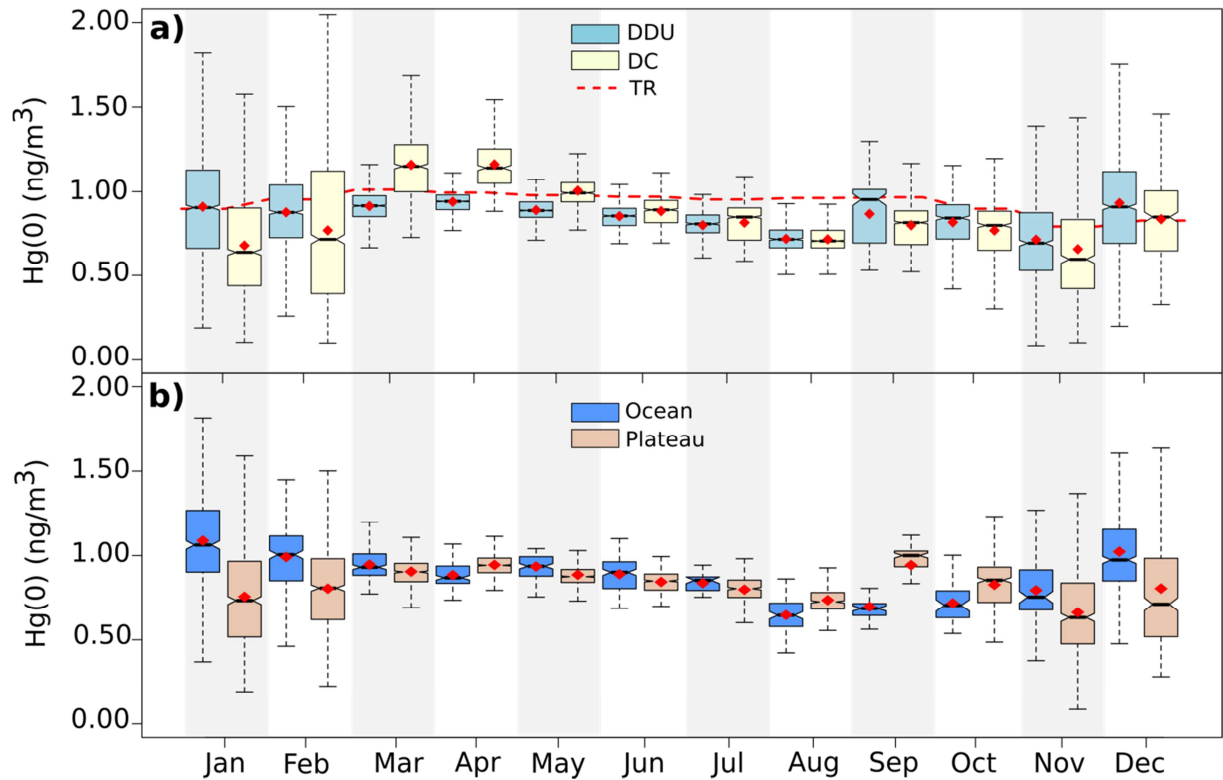


Figure 3: Box and whisker plot presenting the monthly Hg(0) concentration distribution **a)** from all the data collected at DDU and DC along with the monthly mean recorded at TR, and **b)** from all the data collected at DDU associated with air masses originating from the ocean or the Antarctic plateau according to the HYSPLIT simulations. ♦ mean, bottom and top of the box: first and third quartiles, band inside the box: median, ends of the whiskers: lowest (highest) datum still within the 1.5 interquartile range of the lowest (upper) quartile. Outliers are not represented.

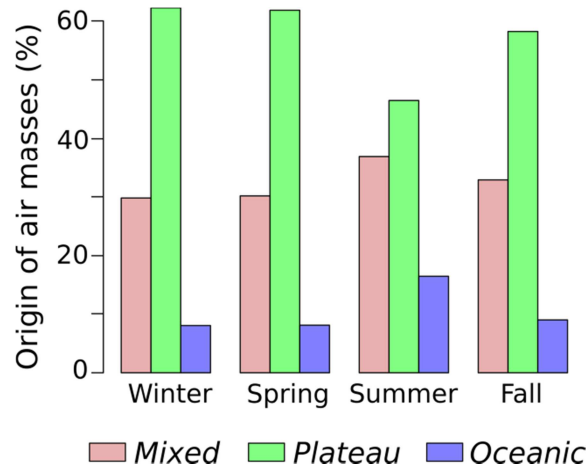


Figure 4: Mean percentage (%) of continental/oceanic mixed air masses (pink), and of air masses originating from the Antarctic plateau (green) or the ocean (blue) according to the HYSPLIT model simulations in winter (May to August), spring (September-October), summer (November to February), and fall (March-April).

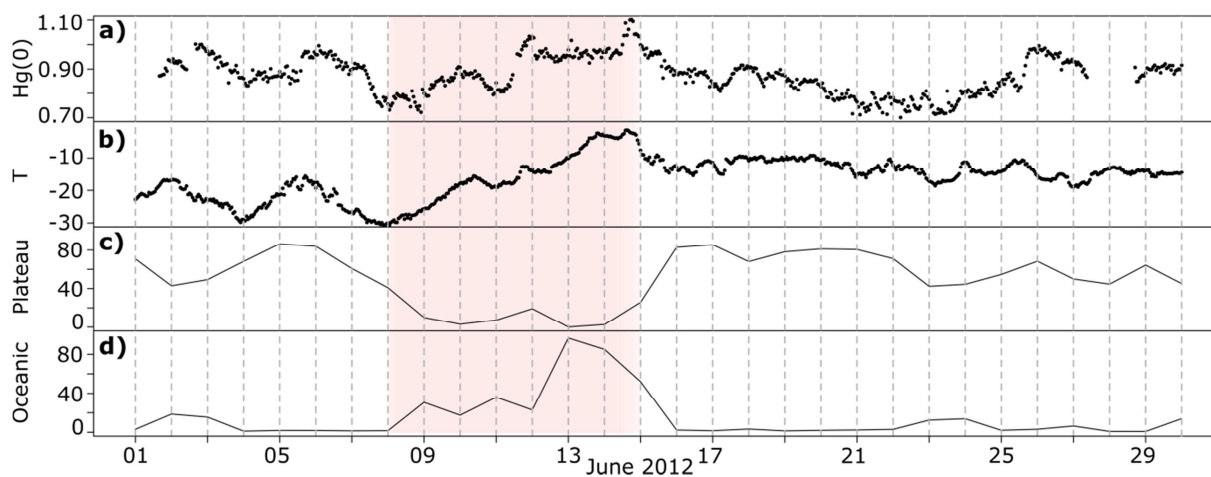


Figure 5: June 2012 variation of **a)** Hg(0) concentration (ng/m^3), **b)** temperature ($^{\circ}\text{C}$), **c)** daily-averaged percentage (%) of air masses originating from the Plateau (HYSPLIT model simulations), and **d)** daily-averaged percentage (%) of air masses originating from the ocean (HYSPLIT model simulations). From 8 to 14 June (period highlighted in red), both Hg(0) and temperature increased suggesting an advection of air masses from mid-latitudes, as confirmed by an elevated percentage of oceanic air masses.

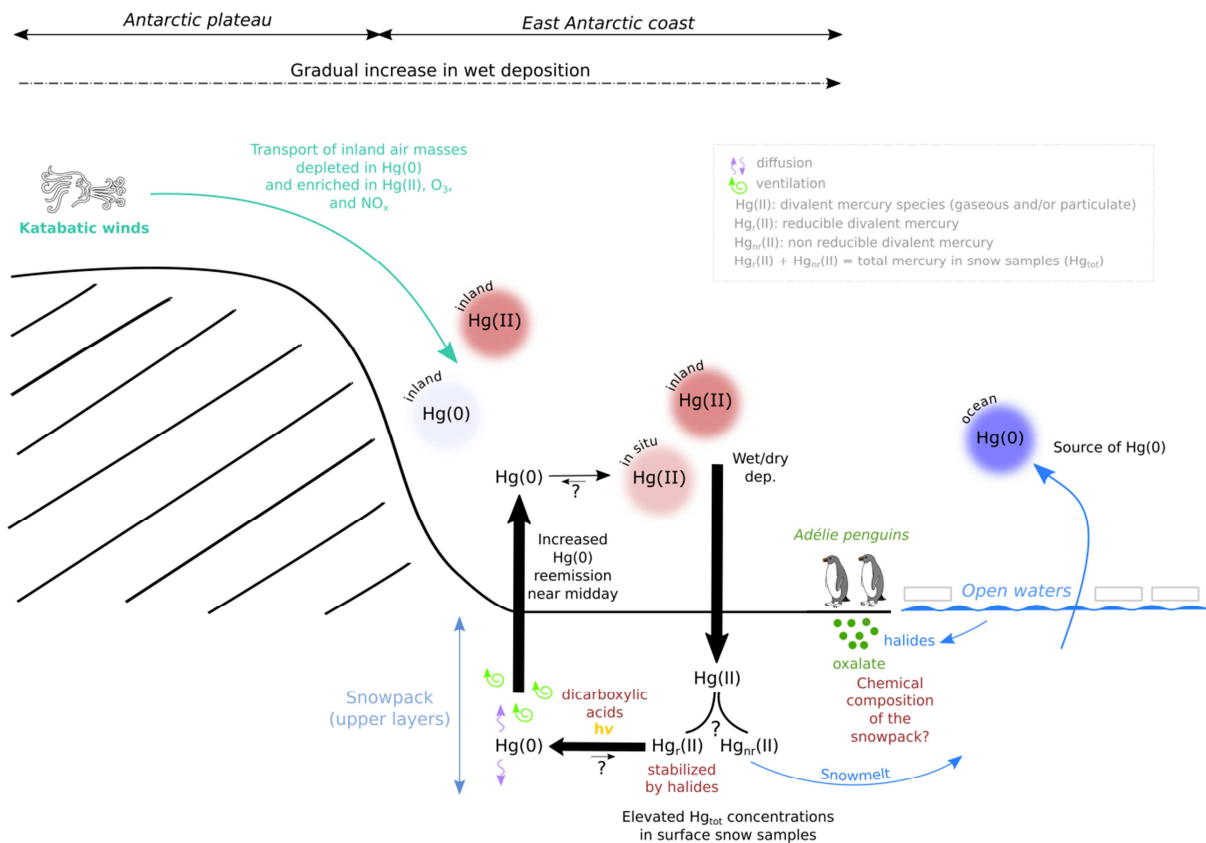


Figure 6: Schematic diagram illustrating the processes that may govern the mercury budget at DDU in summer. Katabatic winds transport inland air masses enriched in oxidants and Hg(II) toward the coastal margins. Hg(II) species deposit onto the snowpack by wet and dry processes leading to elevated concentrations of total mercury in surface snow samples. A fraction of deposited mercury can be reduced (the reducible pool, Hg_r(II)) in the upper layers of the snowpack and subsequently reemitted to the atmosphere as Hg(0). Hg(0) emission from the snowpack maximizes near midday likely as a response to daytime heating. The chemical composition of the snowpack (halides, dicarboxylic acids) may influence the reduction rate of Hg(II) species within the snowpack. The ocean may be a net source of Hg(0) to the atmosphere.

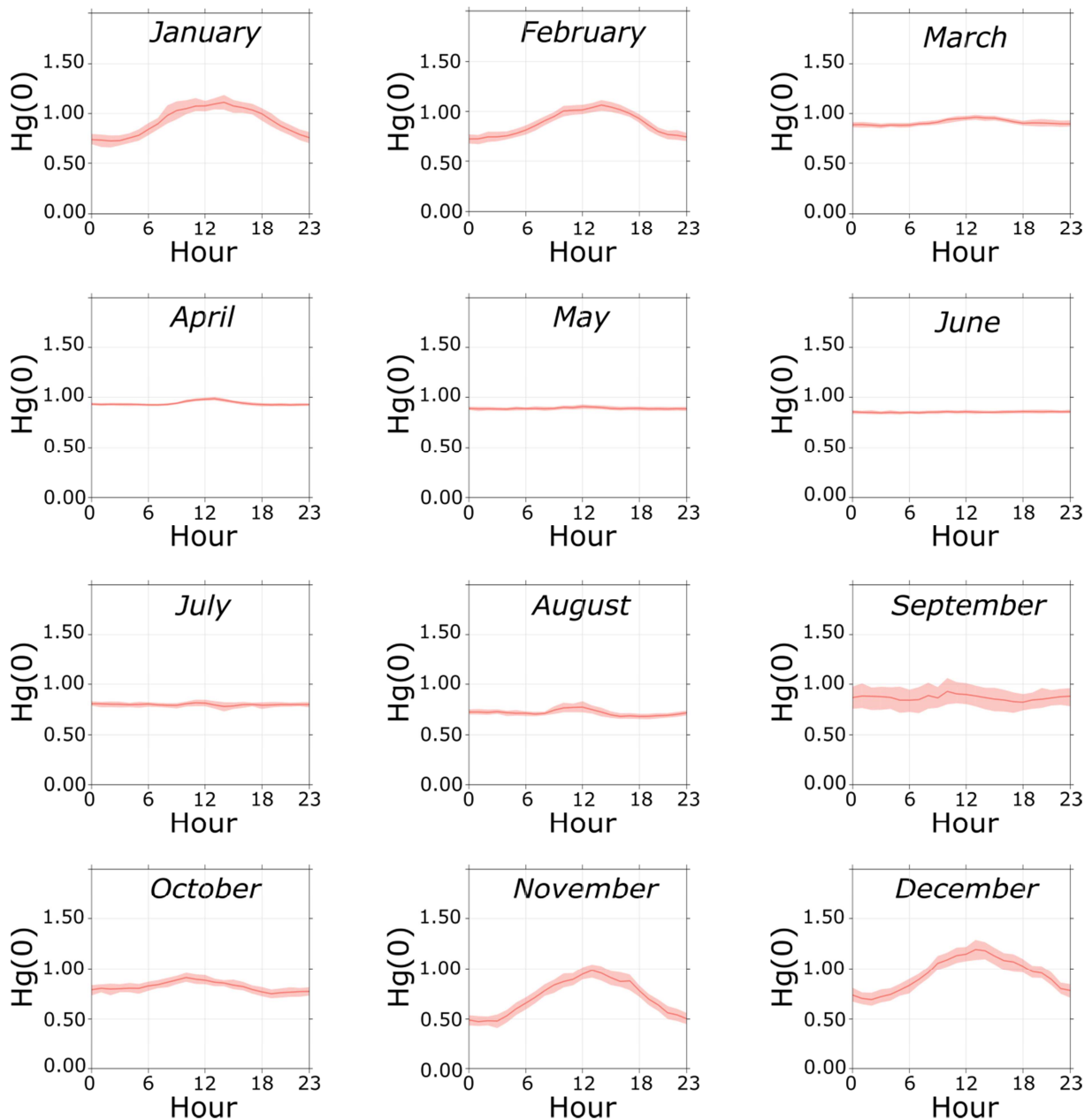


Figure 7: Monthly mean diurnal cycle of Hg(0) concentrations (in ng/m^3) along with the 95% confidence interval for the mean, calculated from all the data collected at DDU (January 2012-May 2015). Hours are in local time (UTC+10). Hg(0) concentrations exhibit a strong diurnal cycle in summer (November to February).

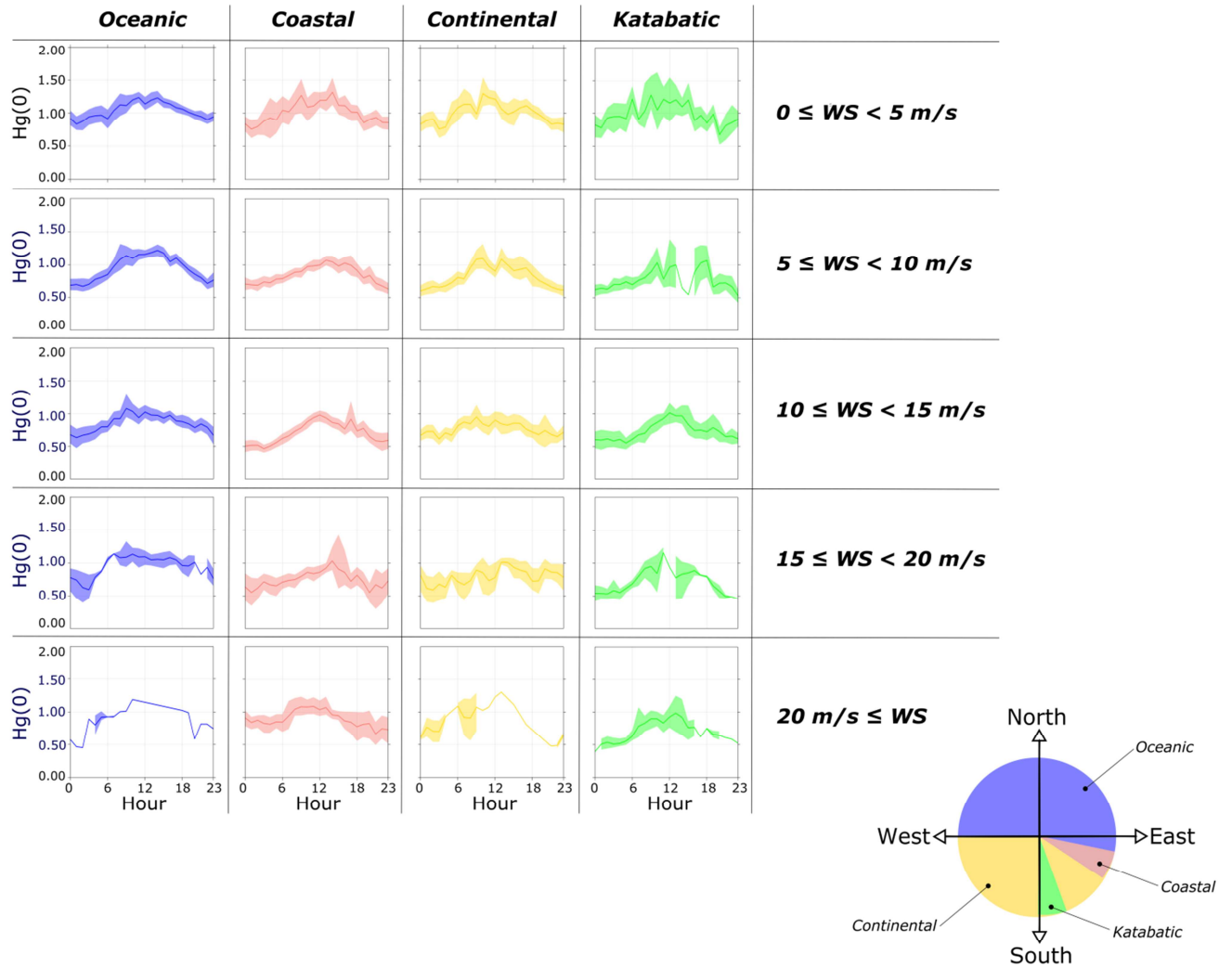


Figure 8: Summertime (November to February) mean diurnal cycle of of Hg(0) concentrations (in ng/m^3), along with the 95% confidence interval for the mean, depending on wind direction and wind speed. With north at 0° , oceanic winds ranged from 270 to 110° , coastal winds from 110 to 130° , katabatic winds from 160 to 180° , and continental winds from 130 to 160° and from 180 to 270° . Hours are in local time (UTC+10). Hg(0) concentrations exhibit a diurnal cycle regardless of wind speed and direction.

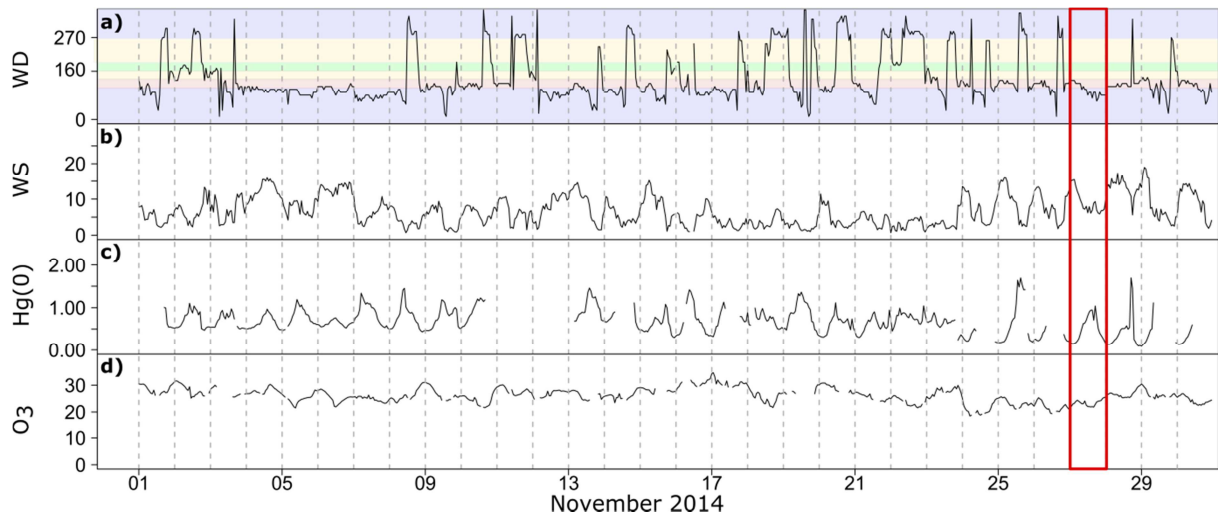


Figure 9: November 2014 variation of **a)** wind direction (WD, in $^{\circ}$), **b)** wind speed (WS, in m/s), **c)** Hg(0) concentration (in ng/m^3), and **d)** O₃ mixing ratio (in ppbv). With north at 0° , oceanic winds ranged from 270 to 110° (purple), coastal winds from 110 to 130° (pink), katabatic winds from 160 to 180° (green), and continental winds from 130 to 160° and from 180 to 270° (yellow). On 27 November 2014 (period framed in red), a sea breeze is observed around midday: WD changes from ~ 120 - 130° to below 110° while WS decreases. Both Hg(0) concentrations and O₃ mixing ratios are not higher than during the previous days.

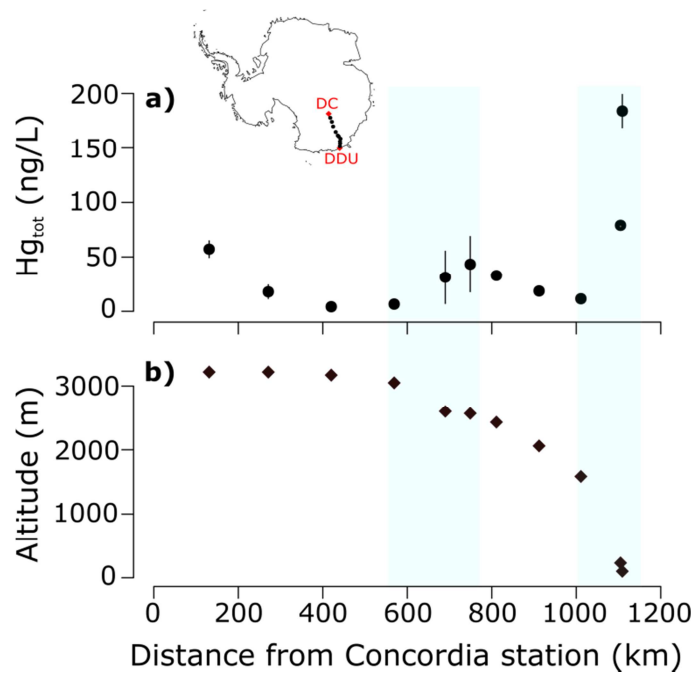


Figure 10: a) Total mercury concentration in surface snow samples (Hg_{tot} in ng/L) along with standard deviation and **b)** altitude (m) vs. distance from Concordia station (DC) during the traverse from DC to DDU. Hg_{tot} concentrations increased in areas highlighted in blue, characterized by steeper slopes and higher snow accumulation values.